

Competing electronic states in high temperature phase of NaTiO₂

Monika Dhariwal¹, L. Pisani² and T.Maitra^{1,*}

¹Department of Physics, Indian Institute of Technology Roorkee, Roorkee- 247667, Uttarakhand, India

²via Salvo d'Acquisto 6, 62017 Porto Recanati (MC), Italy

E-mail: tulimfph@iitr.ac.in(*corresponding author)

Abstract. First principle density functional theory (DFT) calculations on the high temperature phase of layered triangular lattice system NaTiO₂ have revealed that there exists a collective electronic state energetically close to the ground state but with competing transport properties: the latter is metallic with partially occupied doubly degenerate e'_g orbitals whereas the former is insulating with a_{1g} orbital fully occupied. Significant occupation of this excited state is possible at non zero temperature either thermally or thanks to very soft (large amplitude) oxygen vibrations. Possible explanations of the experimental low conductivity based on competing orbital transport and of the specific heat jump at a structural transition based on orbital entropy are discussed.

PACS numbers: 71.20.-b, 71.30.+h, 71.27.+a

1. Introduction

Frustrated magnetic systems with active orbital degrees of freedom have drawn a lot of attention recently among the condensed matter community because of their potential in applications such as spintronics[1]. Two classes of systems that are extensively studied in this context are magnetic spinels having transition metal ion in a pyrochlore lattice [2, 3, 4, 5] and layered materials with transition metal ion forming a two dimensional triangular/hexagonal lattice[6, 7, 8]. Recent experiments[7, 9] and theoretical calculations[10, 11] have shown that orbital ordering in these systems play a major role in lifting the geometrical frustration (often via a structural transition) and driving a (often unconventional) magnetic order as temperature is lowered. At high temperatures, when the lattice is completely frustrated there is a possibility of having competing electronic states. If such states are accessible by tuning an external parameter such as pressure, temperature or magnetic field, one can consider using the system as a switch or memory device in spintronics/electronics applications.

The high temperature phase of NaTiO_2 seems to be a promising candidate in this context as we infer from our detail electronic structure calculations (discussed below). We observe the presence of two distinct electronic states in this system; one is insulating with a_{1g} orbital fully occupied and the other is metallic with partially occupied doubly degenerate e'_g orbitals and these two states are found to be very close by in energy.

NaTiO_2 in its high temperature phase has rhombohedral symmetry (space group $R\bar{3}m$). The two dimensional layer of Ti ions has six equidistant nearest neighbours having Ti-Ti bond length 3.045 Å. Each Ti ion is surrounded by six equidistant O-ions forming TiO_6 octahedron with Ti-O bond lengths being 2.078 Å. Furthermore, these TiO_6 octahedra have a trigonal distortion as O-Ti-O angles deviate from 90 degrees. The three dimensional structure of NaTiO_2 is formed by the stacking of layers of NaTiO_6 -Na. These two dimensional layers of Ti ions form a triangular lattice in the x-y plane and the z-axis (trigonal axis) passes through the centroid of O-triangles above and below the Ti layer. The x and y-axes point towards the next nearest neighbour Ti ions and nearest neighbor Ti ions respectively. The interlayer Ti-Ti distance is about 6 Å and is much larger compared to the intralayer Ti-Ti distance. Hence the system can effectively be considered a two dimensional layered system.

2. Methodology

We have taken the experimental structure of NaTiO_2 in its high temperature phase from Clarke et al. [6]. We have performed a detail electronic structure calculation for the rhombohedral phase of NaTiO_2 using standard full potential linearized augmented plane wave method which is implemented in WIEN2k code[12]. For the experimental structure, the muffin tin sphere radii were chosen to be 2.23, 2.07 and 1.83 a.u. for Na, Ti and O respectively. Plane wave cutoff parameter $R_{mt}K_{max}$ was chosen as 7.00 and approximately 120 k-points were used over the irreducible first Brillouin zone.

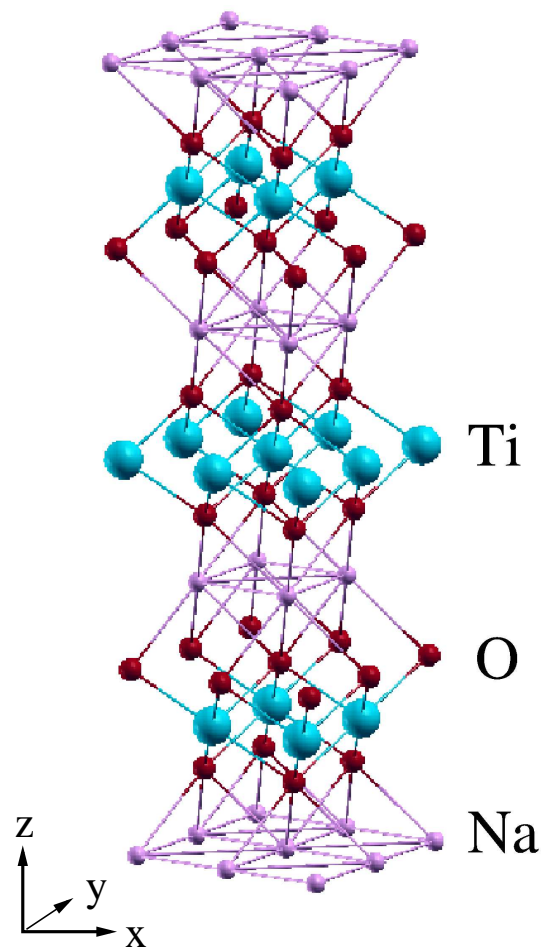


Figure 1. Crystal structure of NaTiO_2 showing layered triangular lattice formed by Ti ions.

Convergence has been achieved to energy values less than 1 meV per formula unit with respect to the variation of number of k-points and the parameter RK_{max} .

As NaTiO_2 contains a transition metal ion having one d electron in the outermost shell, Coulomb correlations are expected to be significant in this system. Therefore, we have performed calculations within local spin density approximation (LSDA) and the LSDA+U approximation (which includes orbital Coulomb correlation). More than one implementation is available for the latter method generating different double counting corrections for the underlying LSDA functional. For moderately correlated (or metallic) systems a mean field approximation to the d-orbital part of the LSDA functional is considered to be appropriate. This is described in details as the Around Mean Field (AMF) functional in ref.[13]. As NaTiO_2 is observed to be a bad metal in both high and low temperature phase experimentally[6], we have chosen the AMF method in our LSDA+U calculations reported below. In this work we consider a range of U values (3.3 - 4 eV) with emphasis on two in particular: 3.6eV and 4.0eV. The former is obtained theoretically via constrained LDA calculations by the authors of ref.[15], specifically for

this compound. This value is very close to that used ($U=3.3\text{eV}$) for compounds like TiOCl , $\text{NaTiSi}_2\text{O}_6$, $(\text{La},\text{Y})\text{TiO}_3$ which gives good agreement with experimental data like magnetic susceptibility[16], spin gap [17], optical measurements [18], respectively. Therefore we take it as a physically reasonable value. The latter is considered merely for theoretical purposes.

3. Results and Discussion

3.1. Experimental structure: ground state

We first study the electronic ground state of the experimental crystal structure within the LSDA and LSDA+U functionals. Fig. 2 shows the electronic band structure within LSDA. The ground state is found to be metallic with Ti d states present at the Fermi level in both spin directions. One also observes that after the octahedral crystal field splitting only t_{2g} states lie at the Fermi level. These are then further split due to the trigonal crystal field of oxygens into two sub-manifolds: e'_g and a_{1g} , the former being doubly degenerate.

In the system xyz of Fig. 1 these orbitals have the following representations (see ref. [20]) based on canonical d-orbitals,

$$\begin{aligned} a_{1g} &: 3z^2 - r^2 \\ e'_g &: 1/\sqrt{3}[yz + \sqrt{2}xy] \\ & \quad 1/\sqrt{3}[zx - \sqrt{2}(x^2 - y^2)] \end{aligned}$$

The a_{1g} orbital has the typical d_{z^2} shape along the trigonal axis and perpendicular to the Ti plane (see Fig. 3); as a result the a_{1g} - a_{1g} direct overlap of σ type is very small. Direct overlap is mainly of π type generating a small bandwidth ($\sim 0.6\text{eV}$) as evident from Fig. 2. The electron density in real space with a_{1g} orbital occupied at all Ti sites is shown in Fig. 3. The negligible a_{1g} - a_{1g} direct overlap of σ type is clearly evident from Fig. 3.

The e'_g orbitals are doubly degenerate and have 4 different contributions from the canonical d orbitals. The xy and $x^2 - y^2$ components have maximum amplitude within the xy plane ($z = 0$) and generate an almost circularly symmetric density providing distributed overlap over all six coordinating Ti atoms. Their direct overlap is of σ type (therefore much stronger than the a_{1g} - a_{1g} overlap) and produces an efficiently delocalising wave function. This is reflected in Fig. 2 by the bandwidth of the e'_g bands of almost 2 eV. The yz component has all 4 lobes π -bonding along the y axis where the Ti-Ti distance is shortest. The xz component has only two lobes remaining from its linear combination with $x^2 - y^2$ within the xz plane: the two pointing towards the oxygen (direction $z = \sqrt{2}x$) vanish and the two pointing in between the other two oxygens are conserved.

From band structure analysis we see that the bands cutting the Fermi level have predominantly e'_g character. In particular the yz component is present in the lowest

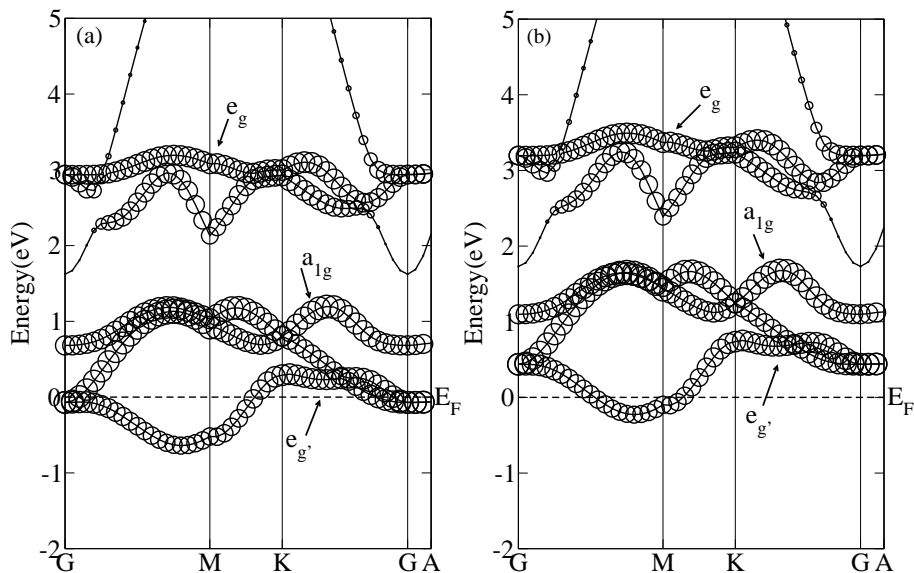


Figure 2. Band structure in both (a) spin up and (b) spin down channel for experimental structure within LSDA.

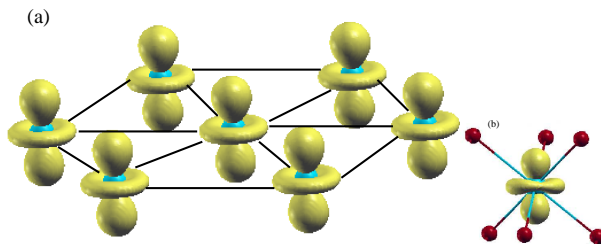


Figure 3. The real space electron density (a) in the Ti plane showing the a_{1g} orbital at each site and (b) within the oxygen octahedron.

band and the xy and $x^2 - y^2$ components in the next one. The highest band of the t_{2g} group has mainly a_{1g} character.

In Table 1 we present electron population analysis within LSDA i.e. the occupation numbers of the t_{2g} bands up to the Fermi level (excluding the valence band contributions due to bonding). As mentioned above, we note that the occupied bands (labelled e'_g in Fig. 2) have a non negligible character of type a_{1g} . This is due to the significant trigonal distortion of the oxygen octahedron which causes the mixing of the two t_{2g} subgroups. The LSDA functional however predicts a slight predominance of e'_g over a_{1g} occupation (for comparison the former should be divided by two due to its degeneracy). This is explained by the fact that e'_g states allow the hopping of electrons over a dense 2d triangular network of Ti atoms (high coordination number and effective orbital overlap in contrast to analogous compound like f.i. TiOCl [14]) thus generating a significant energy gain due to electron delocalisation. Since they are doubly degenerate and not fully occupied (1 electron per Ti atom) the electronic structure is metallic.

	a_{1g}	e'_g
spin up	0.17	0.40
spin dn	0.05	0.08

Table 1. LSDA orbital occupation numbers of the trigonal projections within t_{2g} manifold.

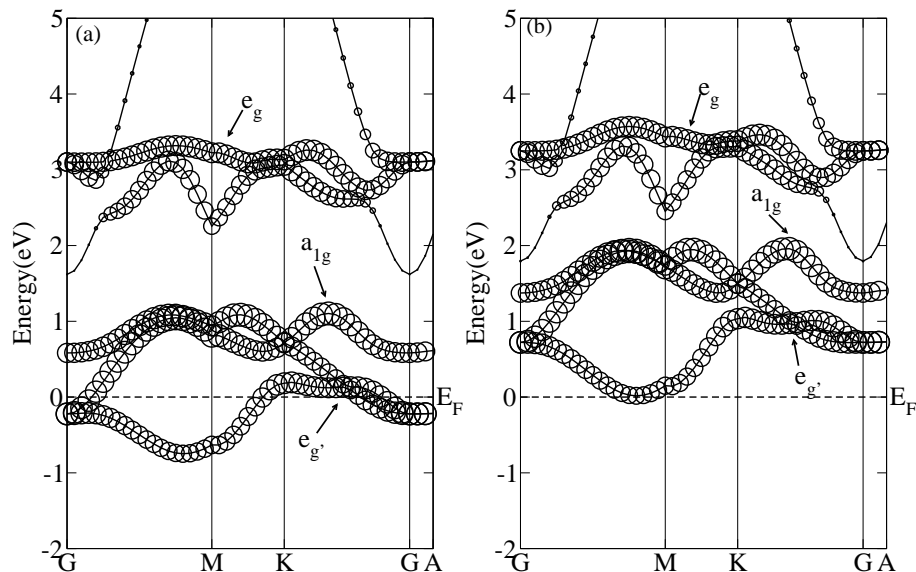


Figure 4. Band structure in (a) spin up and (b) spin down channels within LSDA+U with $U = 3.6$ eV.

For transition metal atoms like Titanium the effect of local electron correlation U is analysed via the LSDA+ U functional. Fig. 4 shows the band structure in both majority and minority spin channels for a physically reasonable value of $U = 3.6$ eV for Titanium[15]. The effect here consists merely in a complete spin polarisation of the bands. Due to the degeneracy of the e'_g states at the Fermi level, no further orbital polarization could be induced by the orbital Coulomb correlation U within LSDA+ U approximation. Therefore, the two majority spin bands remain half filled and the system behaves as a metal.

From Table 1 we note that the occupation number of the a_{1g} orbital is smaller but rather close to the e'_g one (divided by two due to its degeneracy). This suggests that the electronic excitation with a_{1g} orbital occupied is a low energy one. In order to estimate the magnitude of this excitation energy, we took the approach of orbital locking. In this approach, the occupation of a chosen orbital is kept fixed till convergence and then relaxed within a second convergency run. The orbital occupation is fixed by manually setting the initial density matrices (see appendix for details). We call the electronic configuration with a_{1g} orbital occupied predominantly as ES1 state and that with e'_g orbital occupied predominantly as ES2 state, hereafter. Note that for $U=3.6$ eV ES2

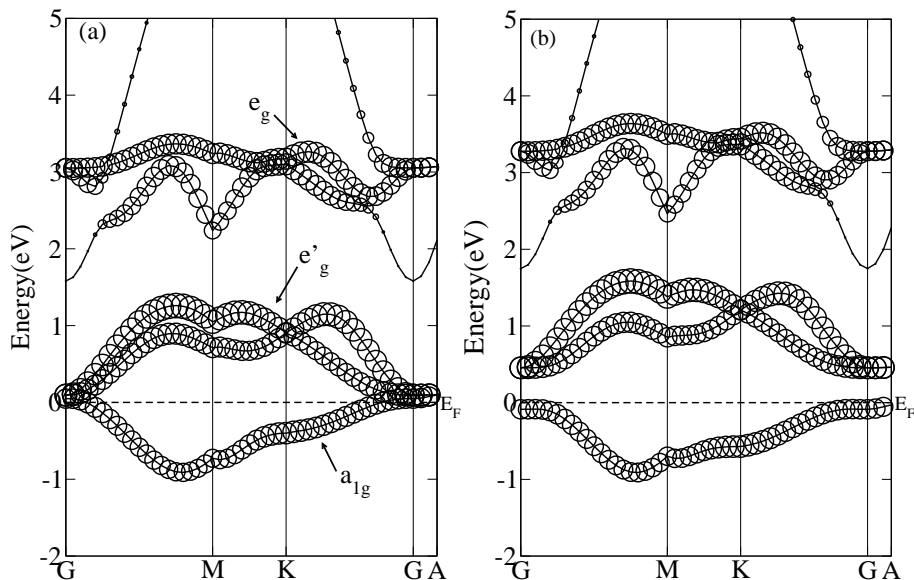


Figure 5. Band structure for ES1 state (see text) in majority spin channel within LSDA+U with (a) $U=3.6$ eV and (b) $U = 4$ eV.

is the ground state. By forcing the single Ti d-electron to occupy the a_{1g} orbital and then allowing it to relax (ES1) we obtain a stable solution with a total energy about 5meV (per formula unit) higher than the ground state one (Fig. 5), using $U=3.6$ eV. This state represents a collective excited state and its electronic structure is illustrated in Fig. 5 (a). It shows the feature of an almost zero gap semiconductor therefore having extremely limited conductivity.

Increasing U to a theoretical value of 4 eV, the ES1 state becomes the ground state whereas ES2 is now an excited state by a tiny energy difference (see next discussion on dependence on U). Fig. 5 (b) shows the ES1 state with a single a_{1g} band below the Fermi level and the opening of a gap in the majority spin channel due to a stronger U . In comparison to previous U value, here the conductivity is totally absent.

Based on this result and given the proximity in energies of the ES1 and ES2 states we study their stability as DFT solutions with varying U . This is obtained using the approach of orbital locking as mentioned earlier. The plot of the resulting total energy difference of the two solutions is presented in Fig. 6. We see that for U values in the region considered physically reasonable for Titanium (around 3.6eV) the ES2 state is the ground state but lower in energy from the ES1 state by only about or less than 5 meV (this is well above the error bar mentioned in the methodology section). As U crosses the value 3.7 eV, ES1 becomes the ground state with the gradual opening of a gap. For $U=4$ eV the gap magnitude in the majority spin channel amounts to about 0.4 eV (see Fig. 5(b)).

The above results show the interplay between two standard and competing mechanisms (energy scales) in transition metal compounds: the localisation (U) favoring

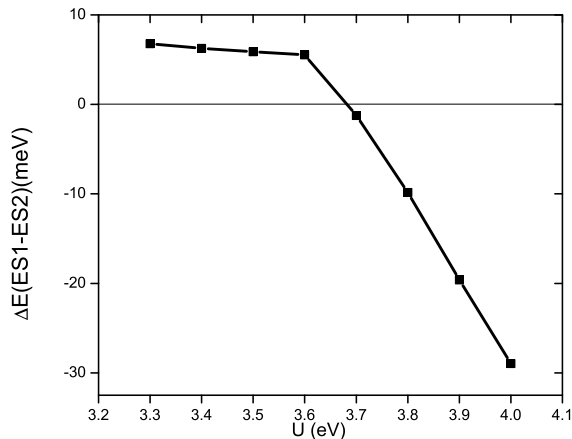


Figure 6. Total energy difference between ES1 and ES2 states with varying U

a_{1g} occupation and the delocalisation (kinetic energy) favouring e'_g . This holds for a wide range of temperatures up to room temperature but for very low temperature ($< 5\text{meV} \simeq 50\text{ K}$) the excited state cannot be thermally reached and only the e'_g state is populated.

For the physical value of $U=3.6\text{eV}$ our results are inline with experimental results by Clarke [6] whereby a bad metal with low but non zero conductivity is found. The bad metallic behaviour is ascribed to the existence of an almost insulating state ($\text{ES1}, a_{1g}$) very close in energy (5meV) to a conducting ground state ($\text{ES2}, e'_g$).

Previous calculations on the high temperature phase of this system was reported in reference [15] where the authors found an insulating behaviour within the LSDA+ U ($U=3.6\text{eV}$) approximation with a spin-polarised a_{1g} band being fully occupied and a gap of about 1 eV. Though we observe the insulating ES1 state as ground state for higher U values ($U > 3.7\text{eV}$), for $U=3.6\text{eV}$ we clearly see that ES2 state is the ground state. More importantly, we observe that these two electronic states (ES1 and ES2) have very closeby energies over a reasonably large range of U values (see Fig. 6).

We would also like to mention that in the calculation reported in reference [15], already within LSDA the a_{1g} occupation was obtained to be higher than that of e'_g which is opposite to what we observe here (see table 1). We believe that this discrepancy is due to the adoption of the Linear Muffin Tin Orbital (LMTO) basis set in the previous calculations contrary to Linearized Augmented Plane Wave (LAPW) basis used here. LMTO is known to be deficient in describing the interstitial region in between atomic (muffin tin) spheres with respect to the LAPW method (see sec. III of ref. [18] as an example). The appropriate description of this region is fundamental to take into account electron delocalization effects via a realistic overlap of the orbitals of e'_g symmetry. Finally, ref. [15] finds the compound to be insulating in contrast to experimental results [6]. Hence the results presented in this work better describes the

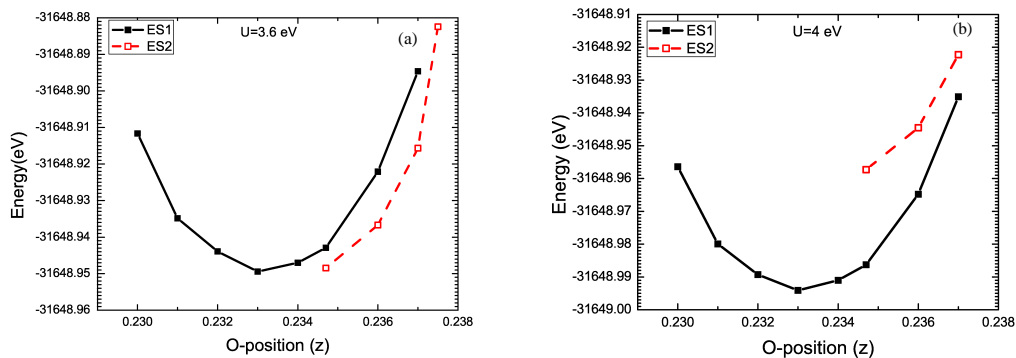


Figure 7. Total energy as function of oxygen coordinate for ES1 (full curve and squares) and ES2 (dashed curve and empty squares) states for (a) $U=3.6\text{eV}$ and (b) 4eV .

experimental situation.

3.2. Lattice effects: optimization of oxygen position

Following an ab-initio approach we investigate the equilibrium structure within the high temperature phase symmetry which allows only for oxygen displacements along the z -axis (Fig. 1). Given the low dimensionality of the problem, we choose to optimize the oxygen positions using the total energy minimization method which is based on drawing the energy curve as a function of the oxygen coordinate (z, z, z) [14]. Lattice parameters are kept at their experimental values. This has the advantage of simulating the effect of van der Waal's forces between layers given that they are not taken into account within DFT. As learnt in previous section, the system presents two almost degenerate groundstates for relevant U values: ES2 (ground state) and ES1 (low lying excited state). Therefore we study the stability of both states as a function of the oxygen coordinate applying the orbital locking method as in previous section.

In Fig. 7 we present the results for two values of U . The full curve represents the total energy of ES1 state and the dashed one is that of ES2 state. For the theoretical U ($=4\text{eV}$) (fig. 7b) the ES1 state is much lower in energy than the ES2 one and represents the groundstate for all oxygen positions. (Note that the ES2 state is not stable for all oxygen positions, as indicated by the dashed curve having no value below the experimental z ($=0.2348$). This is probably due to the crystal field of oxygen atoms preventing the electron delocalisation within ES2 state.) However, for the physical U (3.6eV) (fig. 7a) the energies of ES1 and ES2 become comparable for several oxygen positions. As a consequence there exists a range of oxygen positions ($0.233, 0.235$) for which the total energy is almost constant. As a result oxygen thermal vibrations would be characterised by large amplitudes and generate pronounced orbital fluctuations between a_{1g} and e'_g states.

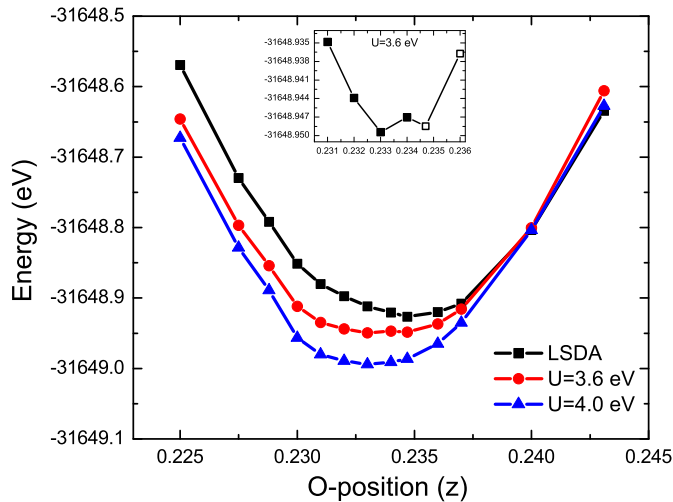


Figure 8. Total energy versus oxygen positions within LSDA and LSDA+U. Oxygen position z is given in fractional coordinate. $z_{exp}=0.2348$ corresponds to the experimental structure. Smaller values of z represent shorter Ti-O bond length. Inset shows a closer view of the energy landscape near the equilibrium point for $U=3.6$ eV; empty symbols represent ES2 state and full ones ES1 state.

The overall energy landscape for three values of U is shown in Fig. 8. Within the LSDA functional ($U=0$), the experimental structure is found to be the equilibrium one. On the contrary for the physical U (3.6eV), the energy landscape is clearly flat as it is for $U=4$ eV but to a lesser degree. In the inset, a zoom-in of the energy curve for $U=3.6$ eV is given showing quantitatively the flatness of the energy curve: its variation remains below 20 meV in a wide range of z values (0.231, 0.236). At room temperature this landscape gives rise to soft oxygen vibrational modes with quite large oscillation amplitudes which enhance orbital fluctuations significantly.

It is worth mentioning that the optimization of lattice parameters does not alter the conclusions drawn above qualitatively. For example, optimization within LDA leads to reduction in both a and c parameters by about 2%. The reduction of a causes a greater overlap of e'_g orbitals thus making ES2 more stable. Competing to this is the shrinking of c which favours ES1 (a_{1g}) due to the crystal field of oxygen being closer to e'_g orbitals.

We note that the above scenario suggest a possible explanation for the anomalous value of the specific heat jump at the structural transition: this is in fact found to be bigger than the one for pure spin system by Takeda *et. al* [19]. Clarke *et. al* [6] have extracted from Takeda's measurements a value of the entropy change of $7 \text{ J K}^{-1} \text{ mol}^{-1}$. In case of long range antiferromagnetic ordering of $S=1/2$ spins the entropy change should be $R \ln(2S + 1) = R \ln 2 = 5.8 \text{ J K}^{-1} \text{ mol}^{-1}$ [6]. No magnetic long range order is found in this system and short range antiferromagnetic correlations could only

give rise to an entropy change lower than $R \ln(2S + 1)$. This would be even further away from the experimental value of $7 \text{ J K}^{-1} \text{ mol}^{-1}$. In this work we have shown at length the relevance and interplay of orbital degrees of freedom. As there are both experimental and theoretical predictions[7, 10] for long range orbital order (with partial orbital polarization at each site) at low temperatures, the entropy change is expected to be lower but indicatively close to $R \ln(2 * |Orb| + 1)$ where the quantum number $|Orb| = 1$ represents the three orbitals: a_{1g} and e'_g . This upper bound amounts to $9.1 \text{ J K}^{-1} \text{ mol}^{-1}$ which would make the entropy change due to orbital order with partial orbital polarization close to the experimental $7 \text{ J K}^{-1} \text{ mol}^{-1}$.

4. Conclusions

We have performed a detail electronic structure calculation for the high temperature rhombohedral phase of NaTiO_2 . We first study the electronic properties of the (non optimised) experimental structure. The ground state is found to be conducting with e'_g orbital symmetry. At an energy slightly greater than the ground state we find an excited state with a_{1g} orbital symmetry and almost fully insulating. By thermal excitation the latter is populated comparably to the ground state giving rise to an overall low conductivity. This is inline with what found by Clarke et al. [6] in their experiments. Secondly, we study the variation of the above properties with respect to lattice via static distortions of oxygen positions along the trigonal axis. Depending on the oxygen proximity to the Ti plane the a_{1g} (oxygens close to the Ti plane) or e'_g (oxygens distant from the Ti plane) orbitals will be alternately populated. Moreover we find the energy landscape to be rather flat which gives rise to a large vibrational amplitude. This implies that at room temperature the population of a_{1g} or e'_g orbitals will oscillate significantly. The specific heat jump at 250 K detected by Takeda et al.[19] could, therefore, be tentatively accounted for by an entropy contribution coming from orbital degree of freedom rather than spin.

5. Acknowledgement

This work is supported by CSIR, India project grant (ref. no. 03(1212)/12/EMR-II). TM acknowledges I. Singh and A. Taraphder for useful discussions.

6. Appendix

The initial density matrices (5×5) supplied for the ES1 and ES2 electronic state within orbital lock approach are in the basis ($l=-2,-1,0,1,2$) as described below. For ES1 state the diagonal elements of the spin up density matrix are set to (0.0, 0.0,1.0,0.0,0.0) and the remaining matrix elements to zero. Therefore only the d_{z^2} ($l=0$) or a_{1g} orbital is populated. The spin down density matrix is identically zero. For ES2 state we have set the diagonal elements of the spin up density matrix to (0.25, 0.25,0.0,0.25,0.25) and

the remaining matrix elements to zero. Here we considered the simplest occupation spectrum with the a_{1g} orbital empty: this consists in populating uniformly all the remaining harmonics ($l = -2, -1, 1, 2$) therefore both the e_g and e'_g orbitals, counting onto the fact that once the orbital lock is removed self consistency will surely depopulate the e_g orbitals due to their energetics.

7. References

- [1] S. D. Bader, S. S. P. Parkin, Annual Review of Condensed Matter Physics, **1** 71 (2010).
- [2] V. O. Garlea, R. Jin, D. Mandrus, B. Roessli, Q. Huang, M. Miller, A. J. Schultz, and S. E. Nagler, Phys. Rev. Lett. **100** 066404 (2008).
- [3] O. Tchernyshyov, Phys. Rev. Lett. **93** 157206 (2004).
- [4] T. Maitra and R. Valentí; Phys. Rev. Lett. **99** 126401 (2007).
- [5] E.M. Wheeler, B. Lake, A.T. M. Nazmul Islam, M. Reehuis, P. Steffens, T. Guidi and A. H. Hill, Phys. Rev. B **82** 140406(R) (2010).
- [6] S. J. Clarke, A. J. Fowkes, A. Harrison, R. M. Ibberson and M. J. Rosseinsky, Chem. Mater. **10** 372 (1998).
- [7] T. M. McQueen, P. W. Stephens, Q. Huang, T. Klimczuk, F. Ronning, and R. J. Cava, Phys. Rev. Lett. **101** 166402 (2008).
- [8] D. I. Khomskii and T. Mizokawa, Phys. Rev. Lett. **94** 156402 (2005).
- [9] Takaaki Jin-no, Yasuhiro Shimizu, Masayuki Itoh, Seiji Niitaka, and Hidenori Takagi, Phys. Rev. B, **87** 075135 (2013).
- [10] Monika Dhariwal, T. Maitra, Ishwar Singh, S. Koley, A. Taraphder; Solid State Communications, **152** 1912 (2012).
- [11] Ting Jia, Guoren Zhang and Zhi Zeng, Phys. Rev. B **80** 045103 (2009).
- [12] Blaha P., Schwartz k., Madsen G.K.H., Kvasnicka D., and Luitz J. 2001 WIEN2K, edited by K. Schwarz, Technische Universitaet Wien, Austria, 2001.
- [13] M. T. Czyzyk and G. A. Sawatzky, Phys. Rev. B, **49** 14211 (1994).
- [14] L. Pisani and R. Valenti, Phys. Rev. B, **71**, 180409(R) (2005).
- [15] S. Yu. Ezhov, V. I. Anisimov, H. F. Pen, D. I. Khomskii and G. A. Sawatzky, Europhys. Lett. **44** 491 (1998).
- [16] Alexander Seidel, Chris A. Marianetti, F. C. Chou, Gerbrand Ceder, and Patrick A. Lee, Phys. Rev. B **67**, 020405(R) (2003).
- [17] S. V. Streltsov and D. I. Khomskii, Phys. Rev. B **77**, 064405 (2008).
- [18] S. V. Streltsov, A. S. Mylnikova, A. O. Shorikov, Z. V. Pchelkina, D. I. Khomskii, and V. I. Anisimov, Phys. Rev. B **71** 245114 (2005).
- [19] K. Takeda, K. Miyake, K. Takeda, K. Hirakawa, J. Phys. Soc. Jpn. **61** 2156 (1992).
- [20] K. Terakura, T. Oguchi, A. R. Williams, J. Kubler, Phys. Rev. B **30** 4734 (1984).